Micromanipulation of Adhesion of a Jurkat Cell to a Planar Bilayer Membrane Containing Lymphocyte Function-associated Antigen 3 Molecules

Aydin Tözeren,* K-L. Paul Sung,‡ Lanping A. Sung,‡ Michael L. Dustin,§ Po-Ying Chan,§ Timothy A. Springer,§ and Shu Chien‡

*Department of Mechanical Engineering, The Catholic University of America, Washington, DC 20064; ‡Department of AMES-Bioengineering and Center for Molecular Genetics, University of California San Diego, La Jolla, California 92093; and §The Department of Pathology, Harvard Medical School, Boston, Massachusetts 02115

Abstract. Cell adhesion plays a fundamental role in the organization of cells in differentiated organs, cell motility, and immune response. A novel micromanipulation method is employed to quantify the direct contribution of surface adhesion receptors to the physical strength of cell adhesion. In this technique, a cell is brought into contact with a glass-supported planar membrane reconstituted with a known concentration of a given type of adhesion molecules. After a period of incubation (5–10 min), the cell is detached from the planar bilayer by pulling away the pipette holding the cell in the direction perpendicular to the glass-supported planar bilayer. In particular, we investigated the adhesion between a Jurkat cell expressing CD2 and a glass-supported planar bilayer containing either the glycosyl-phosphatidylinositol (GPI) or the transmembrane (TM) isoform of the counter-receptor lymphocyte function-associated antigen 3 (LFA-3) at a concentration of 1,000 molecules/μm^2. In response to the pipette force the Jurkat cells that adhered to the planar bilayer containing the GPI isoform of LFA-3 underwent extensive elongation. When the contact radius was reduced by ~50%, the cell then detached quickly from its substrate. The aspiration pressure required to detach a Jurkat cell from its substrate was comparable to that required to detach a cytotoxic T cell from its target cell. Jurkat cells that had been separated from the substrate again adhered strongly to the planar bilayer when brought to proximity by micromanipulation. In experiments using the planar bilayer containing the TM isoform of LFA-3, Jurkat cells detached with little resistance to micromanipulation and without changing their round shape.

CELL adhesion plays a fundamental role in the development of multicellular organisms, cell motility, and immunological responses (23, 29, 33). In this study we used a micromanipulation technique to determine the direct physical contribution of surface adhesion receptors to antigen-independent T lymphocyte adhesion. In particular, we investigated the adhesion of Jurkat human T lymphoma cells to planar bilayers containing lymphocyte function-associated antigen 3 (LFA-3)[1] molecules.

The interaction of a T lymphocyte with other cells and with extracellular matrices is mediated by an ensemble of surface adhesion molecules. As demonstrated by the strong adhesion of cultured T cells to cells lacking a specific antigen, some T cell adhesion molecules can function independently of the T cell receptor for antigen. Antigen-independent T-lymphocyte adhesion is due to the binding of CD2 and LFA-1 receptors on the T cell to LFA-3 and intercellular adhesion molecule (ICAM)-1 and -2 counter receptors on the target cell, respectively (31, 33). Adhesion molecules CD2 and LFA-3 are both members of the Ig super family and can mediate cell-cell adhesion even in the absence of Mg^{+2} (12, 30). By contrast, LFA-1 is an integrin and requires Mg^{+2} for interaction with its multiple ligands ICAM-1 and ICAM-2.

Purified receptors reconstituted in planar phospholipid bilayers have been used to evaluate the minimal requirements for immunological recognition and adhesion (3, 11, 12, 25). In these experiments, lymphocytes are placed on a horizontal coverslip that has been coated by a planar bilayer containing a given type of counter receptor. A flow chamber can be used to determine the percentage of adhering cells to a substrate as a function of applied fluid shear stress (6, 22, 26, 28). This system has been used to study adhesion of T lymphocytes through CD2 to LFA-3 incorporated in planar bilayers. The development with time of resistance to subsequent shear-induced dislodgement was studied as a function of adhesion receptor density and mobility (6). The mobility of LFA-3 within the artificial lipid bilayer was determined using the method of fluorescence recovery after photobleaching (6). These experiments are useful in characterizing the bulk properties of adhesion for a large number of interacting cells,

1. *Abbreviations used in this paper*: GPI, glycosyl-phosphatidylinositol; ICAM, intercellular adhesion molecule; LFA, lymphocyte function-associated antigen; TM, transmembrane.

but a direct evaluation of contact areas and the cell deformation during detachment is not possible with this system.

More recently, a micromanipulation procedure was developed to quantify the geometry of contact between two adhering cells, the change in cell shape during forced detachment, and the force required for de-adhesion. The lectin-induced adhesion of erythrocytes (16, 17), the adhesion between lipid vesicles (15), and the adhesion between a cytotoxic T cell and its target cell (34, 40) were investigated with this method. The micromanipulation data on the coupling between a cytotoxic T cell and a target cell reflect the contribution of an ensemble of complementary adhesion receptor pairs to the physical strength of T-lymphocyte adhesion. It is desirable to complement such data with information about the physical contribution of a given pair of interacting adhesion molecules to T-lymphocyte adhesion.

In this paper, we used a new micromanipulation technique developed by K-L. P. Sung to determine the adhesive energy density between a cell and a glass-supported planar bilayer membrane containing a given type of purified receptor. It is possible with this procedure to compare the contribution of distinct sets of receptors and counter receptors to the physical strength of adhesion of a particular type of cell-substrate system. A planar bilayer possesses the simplest geometry as a substrate (zero surface curvature) and, thus, yields readily to the analysis of the micromanipulation data. The planar bilayer system utilized here has already proved useful in determining the lateral diffusion coefficients of protein macromolecules within the lipid bilayer (6, 37).

Recent biophysical models of cell adhesion (1, 2, 8, 40, 39) have correlated the macroscopic parameters of adhesion, measured here, with the surface density of adhesion molecules, their binding affinity, and their lateral diffusivity, the parameters that are available for the CD2 LFA-3 interaction considered here (6). A fundamental significance of this novel micromanipulation method is that experimental data can be used in conjunction with the analytical approach to yield information on the micromechanics of cell–cell adhesion.

Materials and Methods

We considered the separation of a Jurkat cell from a glass-supported planar bilayer containing LFA-3. The Jurkat human T lymphoma cell line was selected for its high level of expression of CD2 (1.6×10^5 receptors/cell (27). The culture medium in which the Jurkat cells were suspended was RPMI/10% FCS/25 mM Hepes (pH 7.4).

In the experiments, we used two distinct isoforms of purified LFA-3, which differ in membrane anchorage, one with a transmembrane peptide (TM LFA-3) and the other with a glycosyl-phosphatidylinositol moiety (GPI LFA-3) (13). The GPI LFA-3 was isolated from human erythrocytes by using the method of Dustin et al. (13). The TM LFA-3 was similarly affinity purified from the Epstein-Barr virus transformed B lymphoblastoid JY cell clone 33, a mutant line that does not express GPI-anchored proteins and therefore only expresses the TM isoform of LFA-3 (19). Chan et al. (6) showed that GPI LFA-3 is laterally mobile whereas the TM LFA-3 is practically immobile within the glass-supported planar bilayer. The lateral diffusion coefficient of GPI LFA-3 was found to be $2.3 \pm 1.0 \times 10^{-9}$ cm^2/s with 73 ± 13% fractional recovery at room temperature (21–23°C). The TM LFA-3 was practically immobile with <10% fractional recovery, possibly due to interaction of the cytoplasmic domain with glass.

For our experiments, LFA-3 was reconstituted into egg PC liposomes by using the procedure described by Dustin et al. (11) and Chan et al. (6). The liposomes containing purified LFA-3 were suspended in Tris-saline (25 mM Tris-HCl, 150 mM NaCl, pH 8.0). The liposome suspension was stored at 4°C under nitrogen to minimize the effect of oxidation of lipids.

The planar lipid bilayers were prepared as described in McConnell et al. (25). Briefly, the glass chips ($2 \times 10 \times 0.1$ mm) made by cutting a grade-1 Fisher coverslip were boiled for 30 min in a Linbro 7× detergent/water solution (1:6). The chips were then rinsed in deionized water ~50 times over 1 h. Absolute ethanol was used for the last rinse, and the glass pieces were separated on filter paper to air dry. A single glass chip was then positioned vertically in a round glass chamber by the use of a dissecting microscope and glued to the bottom of the chamber. A 5–10-μl drop of liposome suspension was then added on to the glass chip, and the chamber was covered with moist paper towels to retard evaporation. After 25 min at room temperature (21–23°C), the chamber was flooded with the medium and washed without exposing the chip surface to air.

The planar bilayers formed with the procedure described above are uniform and continuous as shown by incorporation of a fluorescent lipid analogue, NBD-PE, and examination under a Meridian ACAS 570 interactive laser cytometer (6). The planar bilayers formed by the identical procedures in these studies had a uniform appearance in sections of osmium-fixed samples examined with a JEOL 100C/ASID EM (5). The low mobile fraction (<10%) of TM LFA-3 suggests the absence of significant degree of multilayering of the planar bilayer. If the planar bilayer were to consist of multilamellar bilayers, TM LFA-3 would then be expected to be highly mobile since the cytoplasmic domain of TM LFA-3 (only 12 amino acids long) on the top bilayer would not be able to anchor to the glass surface.

The surface density of both isoforms of LFA-3 in the upper leaflet of the planar bilayers was estimated by immunoradiometric assay directly on the planar bilayers formed under identical conditions (6). Both LFA-3 forms are uniformly distributed in the planar bilayer as judged by fluorescence. As shown by Dustin et al. (14), the enzymatically generated soluble extracellular portion of GPI LFA-3 and the detergent-solubilized GPI and TM isoforms of LFA-3 behave as monomers, suggesting no strong tendency to aggregate. In the experiments presented in the next section, the surface density of both isoforms of LFA-3 measured in sites/μm^2 was approximately equal to 1,000 (994 ± 31 for GPI LFA-3 and 1,069 ± 46 for TM LFA-3), unless otherwise noted.

A micropipette was mounted on a hydraulic micromanipulator on the stage of an inverted microscope (15). The stickiness of Jurkat cells to the holding pipettes was reduced by filling the micropipettes with the culture medium before experiments. The wide end of the pipette was connected to a pressure regulation system. A Jurkat cell in the micromanipulation chamber was held at the tip of the pipette by the application of a small aspiration pressure (100–500 dyn/cm^2). The cell was then brought close to a vertical glass-supported planar bilayer reconstituted with a given type of purified adhesion receptor. The negative pressure in the holding pipette was removed and the cell was allowed to interact with the planar bilayer for 5–10 min.

After the completion of the period of incubation, a Jurkat cell adhering to the planar wall was captured by the micromanipulation of the pipette with a small aspiration pressure. The pipette was positioned at all times approximately perpendicular to the planar bilayer in order to preserve an axisymmetric cell geometry during peeling. As the pipette was gradually moved away from the planar bilayer, the aspiration pressure in the pipette was increased in small steps to a level that would allow the complete separation of the cell from the planar bilayer. The videotaped sequence of the micromanipulation experiments showed that the aspirated portion of the cell increased in length as the aspiration pressure was increased, and that at low suction pressures the cell slipped out of the pipette. The minimum aspiration pressure that led to the detachment of a Jurkat cell from the receptor-containing planar bilayer was referred to as the critical separation pressure (P).

The micromanipulation events depicting the transient peeling of a cell from its substrate were continuously recorded by using an inverted microscope, a video camera, and a video time-recorder system.

Results

The Deformability of Jurkat Cells

Deformability of the Jurkat cells was assessed by micropipette aspiration (35, 36). The suction pressures used in the experiments ranged from 400 to 900 dyn/cm^2. The length of the resulting cell projection in the pipette was comparable to the pipette radius (1.5–2.5 μm). Micropipette aspiration results were analyzed by using the leukocyte deformability model in which the cell was idealized as a cortical shell encompassing a Maxwell viscoelastic fluid (9, 18). The three

Table I. Jurkat Cell Deformability

Experiment	No. of measurements	Aspiration Pressure	T_o	μ	κ
		dyn/cm²	*dyn/cm*	*dyn-s/cm²*	*dyn/cm²*
Micropipette aspiration	45	643 ± 165	0.086 ± 0.004	35 ± 20	459 ± 219

T_o, Isotropic cortex tension; κ, Elastic coefficient of the cytoplasm; μ, Viscous coefficient of the cytoplasm.

Table II. Detachment of Jurkat Cells from a Planar Membrane Reconstituted with 1,000 LFA-3 Molecules/μm²

Experiment	No. of sites per μm²	R_p	$R°_c$	P	γ
		μm	*μm*	*10^3 dyn/cm²*	*dyn/cm*
GPI LFA-3	1,000	1.5-2.5	2.5 ± 1.5	2.7 ± 1.5	0.06 ± 0.03
GPI LFA-3	100	2.0-3.4	2.5 ± 0.8	0.6 ± 0.4	0.03 ± 0.01
TM LFA-3	1,000	2	1.0 ± 0.6	0.1 ± 0.1	$(4 \pm 3) \times 10^{-4}$ *

R_p, Radius of the pipette; $R°_c$, Radius of the contact region before detachment; P, Critical aspiration pressure; γ, Adhesive energy density. The parameter γ was computed by using the following equation: $\gamma = (PR^2_p/2R_c) \sin\theta\,(1 - \cos\phi)/\sin\phi$ where ϕ and θ are the angles the cell surface makes with the planar membrane at the edge of conjugation and at the tip of the pipette, respectively (17, 40). * The parameter γ was computed by using the equation $\gamma = PR^2/(3\pi R_o)$ where R_o is the radius of the Jurkat cell (20).

parameters of cell deformability deduced from micromanipulation data are the isotropic cortex tension (T_o), the elastic coefficient of the cytoplasm (κ), and the viscous coefficient of the cytoplasm (μ) (Table I). The values of T_o and κ were of the same order of magnitude of those for leukocytes (9), but the value of μ was about an order of magnitude lower.

Jurkat Cells Interacting With Planar Membranes Containing GPI LFA-3

We performed a set of control experiments using glass chips without planar bilayer coating or coated with planar bilayer without protein incorporation. The glass chip, vertically positioned on the bottom of the chamber, was cleaned as before. The cell suspension was introduced into the chamber after the chamber had been washed several times with the medium. The results of these control experiments showed that the Jurkat cells did not adhere to the clean glass surface prewashed with the medium. When the vertical glass chip was coated with a planar bilayer without LFA-3, the Jurkat cells also did not bind to the planar bilayer.

Jurkat cells conjugated strongly with planar bilayers reconstituted with 1,000 GPI LFA-3 molecules/μm². Our experimental measurements on Jurkat cells interacting with LFA-3-bearing planar bilayers are summarized in Table II. The radius of conjugation (R_c) remained essentially constant after the initial 5–10 min of the incubation period; its maximum value in an experiment was denoted as $R_c°$. The results of 43 experiments in which a different cell was brought to a different location on the planar bilayer containing GPI LFA-3 showed that $R_c°$ was equal to 2.5 ± 1.5 (SD) μm. The critical aspiration pressure required to detach these cells from the GPI LFA-3-bearing planar bilayer was (2.7 ± 1.5) × 10^3 dyn/cm². The average diameter of the Jurkat cells used in the experiments was 15 ± 2 μm. An increase in the duration of incubation from 5–10 min to 20–30 min did not result in a significant increase in the critical aspiration pressure.

A typical sequence of micromanipulation events with GPI LFA-3 is shown in Fig. 1. We plotted in Fig. 2 the diameter of the contact area (D_c) and the distance between the planar bilayer and the tip of the pipette (L_c) as a function of time for the micromanipulation events shown in Fig. 1. These figures show that the cell elongated in the direction of the pipette. When the diameter of the contact area decreased by ~50%, the cell detached suddenly from the planar substrate in the second phase that lasted typically less than a second. The contour of the part of the cell previously in contact with the planar bilayer remained flat immediately after detachment. The Jurkat cells that had just been detached from the substrate again adhered strongly to the planar bilayer when brought into proximity by micromanipulation.

The mode of cell detachment from the membrane-coated glass chip is unknown. It is possible that part of the cell membrane most tightly adherent to the membrane-coated glass chip might have been sheared off the cell and remained behind on this planar surface, while the cell quickly resealed itself. If the planar bilayer remained adherent to the underlying glass chip during cell detachment, the separation of the cell from the substrate may have occurred as a result of (*a*) the detachment of CD2 molecules on the surface of the Jurkat cell from LFA-3 molecules on the planar bilayer and (*b*) the extraction of CD2-LFA-3 bonds from either the Jurkat cell membrane or the planar bilayer. Our studies do not allow a differentiation between these possibilities.

A small subgroup of Jurkat cells (4 out of 43 experiments) detached from the planar substrate without a significant change in morphology from their round configuration (Fig. 3). The critical aspiration pressure required to detach a Jurkat cell in the experiments that belonged to this subgroup was (0.7 ± 0.2) × 10^3 dyn/cm². This is approximately fourfold smaller than the mean aspiration pressure for the other Jurkat cells interacting with the GPI LFA-3-bearing planar bilayer. The reason for this variation is unknown and may reflect on the heterogeneity of Jurkat cells and/or the planar bilayer.

Micromanipulation experiments were also conducted on planar bilayers containing ~100 GPI LFA-3 molecules/μm². This surface density of LFA-3 is comparable to the surface density of CD2 molecules on Jurkat cells (125/μm²)

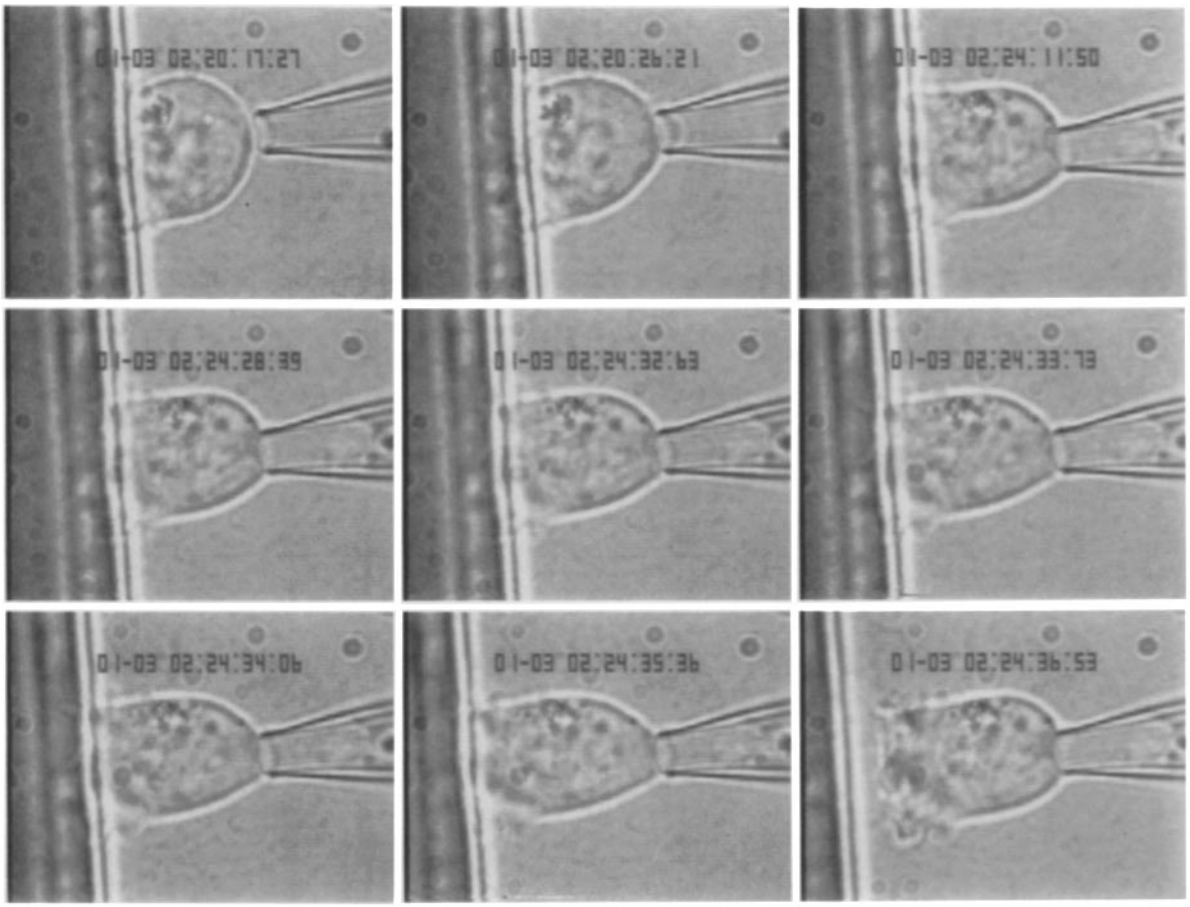

Figure 1. Sequence of photographs showing a typical time course of detachment of a Jurkat cell from a glass-supported lipid bilayer containing 1,000 GPI LFA-3 molecules/μm^2 ($P = 4.5 \times 10^3$ dyn/cm^2 and $R_p = 1.7$ μm). The photographs were taken from the TV monitor and represent the discrete instances of the micromanipulation events observed in an experiment. The numbers on the top of the screen represent, in order, month, day, hour, minute, second, and tens of milliseconds.

(6) and the surface density of GPI LFA-3 on human erythrocytes (50 sites/μm^2) (30). The results of the micromanipulation experiments are shown in Table II. Jurkat cells spread on planar bilayers containing 100 GPI LFA-3 sites/μm^2 during 5–10 min incubation, as in the experiments with 1,000 sites/μm^2. The critical force ($P\ R_p^2$) and the extent of cell elongation before detachment were less than those for experiments with 1,000 GPI–LFA-3/μm^2. These results show the existence of significant binding of Jurkat cells to planar bilayers reconstituted with GPI LFA-3 for a wide range of LFA-3 concentrations.

Adhesion of Jurkat Cells to Planar Membranes Containing TM LFA-3

When the planar bilayer contained TM LFA-3 instead of GPI LFA-3, at the same surface density of 1,000 LFA-3 molecules/μm^2, the adhesion of the Jurkat cell to the planar bilayer was so weak that in many instances it was difficult to measure the contact radius. An increase in the duration of incubation from 5–10 min to 20–30 min did not result in an increase in the contact area. For eight experiments in which the contact area was clearly visible under the microscope, we found that $R_c^\circ = 1.1 \pm 0.6$ μm. The cells that adhered to the TM LFA-3–bearing membrane detached rapidly when the pipette holding the cell was pulled away at comparable speeds. The Jurkat cells preserved their round shape during the course of separation as shown in Fig. 4. The critical aspiration pressure for TM LFA-3 was $(0.1 \pm 0.1) \times 10^3$ dyn/cm^2, which was ~25-fold smaller than the corresponding pressure in GPI LFA-3 experiments. The critical aspiration pressure did not increase significantly when the duration of incubation was increased to 20–30 min.

Discussion

Macroscopic Parameters of Adhesion of a Cell to a Substrate

In applied mechanics, the adherence strength of a body (such as a tape or a beam) to a rigid planar substrate is investigated by measuring the external forces required to detach the body from the substrate. In engineering analysis of peeling and crack propagation, a boundary condition characterizing the breaking of adhesive bonds between a body and a substrate is derived by introducing the concept of adhesive energy density, γ (dyn/cm), i.e., the energy per unit area absorbed at the moving edge of separation (4). In the case of detachment of a flexible but inextensible tape from a planar substrate, the work done by the tension in the tape during peeling is used to break the bonds between the tape and the substrate (4).

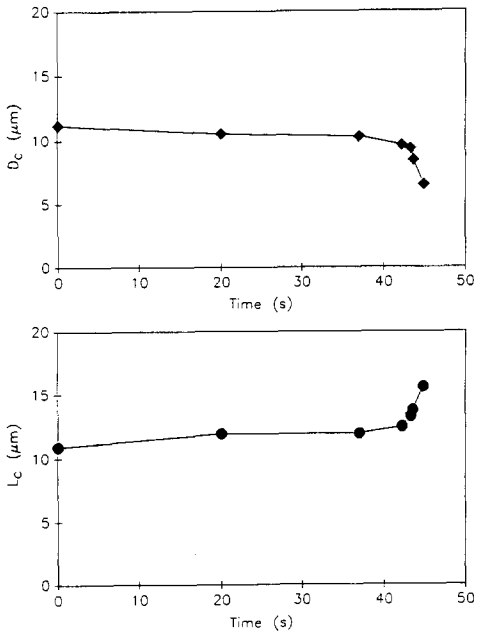

Figure 2. The time histories of the diameter of conjugation (D_c) and the distance between the planar bilayer and the tip of the pipette (L_c) during detachment for the micromanipulation events shown in Fig. 1.

In the case of cell detachment by micromanipulation, the adhesion parameter γ is equal to the meridional membrane tension T_c multiplied by the geometric term $(1-\cos\phi)$ (17, 40). Here, ϕ denotes the angle the cell surface makes with the planar bilayer at the edge of conjugation. It is not possible to measure the meridional cell membrane tension at the edge of conjugation. For this reason, in previous studies of cell adhesion, the parameter T_c was evaluated from micromanipulation data by using the equations of static equilibrium and assuming that the pressure difference between the cell and the surrounding medium was negligible in comparison with the critical aspiration pressure (17, 40). Our computations (not presented here) show that this procedure yields γ values that are practically identical to the ones predicted by a cell model in which the circumferential tension in the cell membrane is negligible in comparison with meridional tension. This is a reasonable approximation for cases in which the cell adhering to the planar bilayer stretches extensively in the direction of the pipette prior to detachment.

Comparison of the Strength of Adhesion between Jurkat Cells and Planar Membranes Containing LFA-3 with That for Various Cell Couples

We computed the value of the adhesive energy density at the initial stage of detachment of Jurkat cells from planar

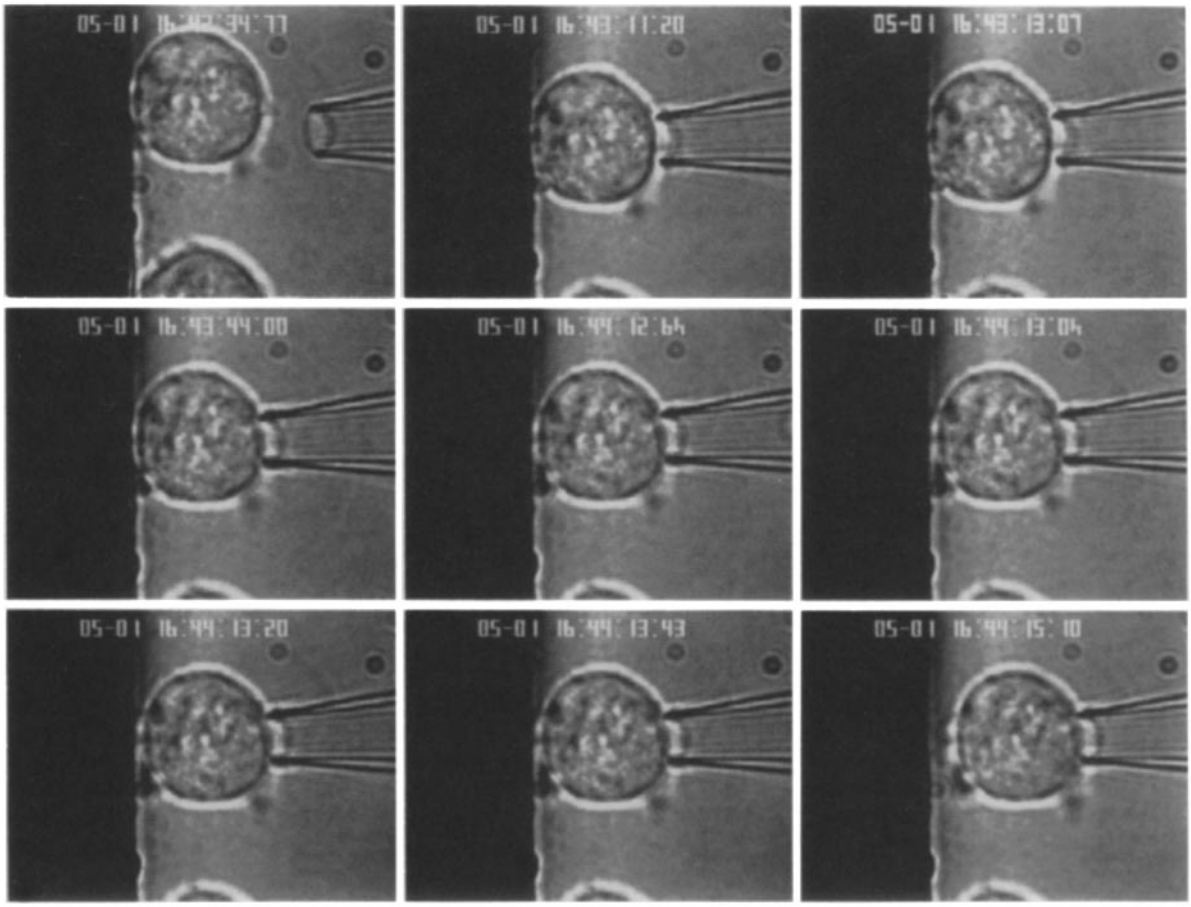

Figure 3. Sequence of photographs showing the micromanipulation of a Jurkat cell adhering relatively weakly to a glass-supported lipid bilayer containing GPI LFA-3 for which $P = 0.7 \times 10^3$ dyn/cm^2 and $R_p = 1.7$ μm.

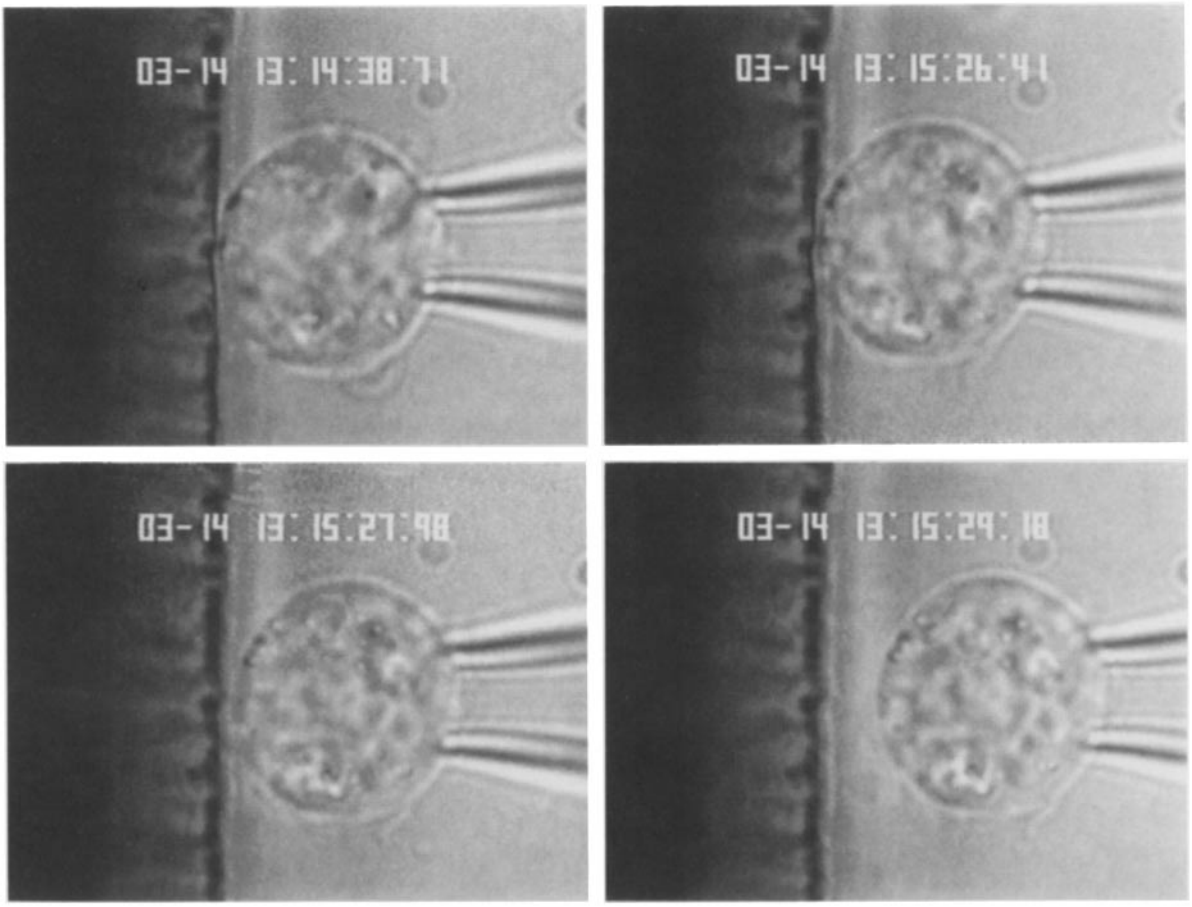

Figure 4. Sequence of photographs showing the time course of detachment of a Jurkat cell from a planar bilayer containing TM LFA-3 ($P = 0.1 \times 10^3$ dyn/cm^2; $R_p = 1.8$ μm).

bilayers containing 100 and 1,000 GPI LFA-3/μm^2 from micromanipulation data by using the equation presented by Evans and Leung (17) (see Table II). This equation may not be valid when the viscous dissipation in the cell becomes important. This may be the case in the final stage of detachment when the contact area decreases and the cell elongates rapidly (Fig. 1). For experiments in which the cell preserved its axisymmetry during detachment, the adhesive energy density (γ) was equal to 0.03 $\pm$ 0.01 dyn/cm for 100 sites/μm^2 and 0.06 $\pm$ 0.02 dyn/cm for 1,000/μm^2. Adhesion energy density is not linearly dependent on the surface density of GPI LFA-3 within the planar bilayer when this density is comparable or greater than the corresponding surface density of CD2 molecules on a Jurkat cell.

Jurkat cells detached from planar bilayers containing TM LFA-3 so quickly that it was not possible to evaluate the geometric parameters required for the computation of the adhesion parameter γ by using the method of Evans and Leung (17). Furthermore, the assumption that the pressure difference between the cell and the medium is small compared to the critical aspiration pressure may not be valid for cells weakly adhering to a substrate. For this reason, the adhesion parameter γ was computed by using the analytical solution for an elastic sphere adhering to a substrate (20). In this formulation the critical force of detachment ($P R_p^2$) divided by ($3\pi\gamma R_o$) is equal to where R_o denotes the radius of the sphere (7.5 μm). This formulation is appropriate for Jurkat cells adhering to TM LFA-3 because even if the Jurkat cells are viscoelastic, their short time behavior is essentially elastic. The adhesion parameter γ computed with this procedure is equal to 0.4×10^{-4} dyn/cm (Table II). This is ~100-fold smaller than that for GPI LFA-3 at the same surface density.

The adhesion parameter γ at the initiation of detachment of a cytotoxic T cell from its target cell is approximately equal to 0.20 dyn/cm (40). This adherence strength is about sixfold greater than that of a Jurkat cell detached from a planar bilayer containing 100 GPI LFA-3/μm^2. This suggests that the reversible interaction of T cell receptor CD2 with its counter-receptor LFA-3 is only one of many factors contributing to the physical strength of adhesion of T cells to their target cells.

A Possible Mechanism for the Rapid Propagation of the Edge of Separation

The rapid detachment of Jurkat cells from planar bilayers containing GPI LFA-3 after they deformed in response to micromanipulation is different from the corresponding detachment of cytotoxic T cells from their target cells (34). As the contact area between a cytotoxic T cell and its target cell reduced gradually towards zero during detachment by micromanipulation, the adhesion parameter γ increased 10-fold (40).

The mechanism of cell detachment shown in Fig. 1 is

reminiscent of the propagation of a crack through a solid. Consider, for example, an infinitely long elastic beam with a partial split of a length λ at one of its ends from a planar substrate to which it adheres. As discussed by Burridge and Keller (4), the split end of the beam will initially be displaced away from the planar substrate without a change in λ in response to a force applied at the split end of the beam in the direction normal to the beam–substrate interface (F). The crack will expand at its tip towards the other edge of the beam only after the beam curvature at this point exceeds a critical value, say K. The parameter K is related to the adhesive energy density γ and the bending rigidity of the beam EI by the simple equation: $K = (2\gamma/EI)^{1/2}$. The stability analysis of this problem shows that the crack will propagate rapidly and catastrophically once the force F acting at the cracked edge of the beam exceeds $(K(EI)/\lambda)$. This is because the elastic bending energy stored in the beam by the force applied at the cracked edge is released during crack propagation and absorbed at the moving boundary.

The fracture solution discussed here shows that the critical normal force that initiates crack propagation increases with increasing adhesive energy density. This may be one reason why crack propagation is not observed during the forced-detachment of T cells from their target cells. The geometry of the Jurkat cell at the time of separation, Fig. 1, is quite different from that of an elastic beam, but the concept of the reason for rapid crack propagation probably applies. Namely, the strain energy stored in the Jurkat cell is released once the critical load is reached, and this energy is rapidly used to propagate a crack.

In the case of the adhering beam, the critical force for initiation of crack propagation is inversely proportional to the initial crack length λ which acts like a lever arm. There is no immediate counterpart of this initial crack length in case of a more or less spherical cell like the Jurkat cell. However, the complement of λ, namely the attached length or contact area is a significant parameter in the cell case. For elastic spheres, it can be shown that there is a critical force and critical area of contact at which rapid separation follows, due to the strain energy release when separation starts.

The Morphology of Jurkat Cells Adhering to Planar Membranes Containing GPI LFA-3

We simulated the cell shapes observed in the micrographs shown in Fig. 1 by using a cell model in the form of an axisymmetric membrane encompassing a fluid-like material. The cell membrane was defined as the plasma membrane and the attached cytoskeletal structures such as the actin-rich cortical shell. In this model, the force exerted by the pipette on the modeled cell is transmitted to the edge of conjugation by the meridional cell membrane tension and the pressure difference between the cell and the medium is assumed to be finite but uniform.

Two particular cases of membrane tension distribution along the cell surface are considered. In model 1, the circumferential cell membrane tension (T_2) is assumed to be negligibly small in comparison with the meridional cell membrane tension (T_c). This model may be reasonable for cases in which the cell undergoes significant extension in the direction of the pipette (e.g., in the majority of the GPI LFA-3 experiments). The load carrying components of the cell membrane (i.e., actin fibers in the cortical shell) will tend to align themselves along the meridional direction as the cell is stretched by the pipette, resulting in an increased meridional tension.

In model 2, we consider the other extreme, namely, the case in which the tension in the cell membrane is isotropic ($T_1 = T_2$). It is expected that this is a reasonable model for lipid bilayer vesicles and for cases in which the deviation from a spherical cell shape is not extensive (e.g., in the small subset of the GPI LFA-3 and all TM LFA-3 experiments).

Fig. 5, column 1, shows the experimental cell contours at three discrete times during the micromanipulation events presented in Fig. 1. The modeled cell contours corresponding to these experimental cell shapes are given in column 2 (model 1) and column 3 (model 2). The figure shows that both models reproduce the general shapes of the cell observed in a micromanipulation procedure, but model 1 consistently predicted more accurately than model 2 the axial length of the deformed cell attached to the GPI LFA-3 bearing planar bilayer.

The model cell contours deviate from the actual cell contours in one respect. As shown in Fig. 4, models 1 and 2 predict cell contours that are always symmetric with respect to a plane that intersects the cell at its largest cross section. The video-micrographs shown in Fig. 1 indicate that this is not a feature observed experimentally. These results suggest that the load sharing mechanism of the cell may be more complex than those described by models 1 and 2. For example, the cell nucleus, being more viscous than the surrounding cytoplasm, may resist the radial deflection of the cell during detachment by micromanipulation. The lack of symmetry may reflect the nonhomogeneity in the interaction of CD2 with LFA-3, which may result from the interaction of CD2 with the cytoskeleton and its inability to diffuse quickly in response to the applied force. Internal cell structures such as microtubules, actin, and intermediate filaments may resist the stretching action of the micropipette so the model of the cell interior in terms of only a constant fluid pressure may not be accurate.

The Effect of LFA-3 Mobility on the Strength of Jurkat Cell Adhesion

The significant difference in adherence strengths of Jurkat cells to planar bilayers containing TM LFA-3 vs. GPI LFA-3 after 5–10 min incubation can not be accounted for by differences in their molecular size or their binding affinity with CD2 or by variations in the nonspecific repulsion between the cell and the substrate (6).

The adhesion of Jurkat cells to planar bilayers containing mobile LFA-3 may gain strength more rapidly than adhesion to membranes containing immobile LFA-3, because the rate of bond formation depends on the local mobility of the interacting adhesion molecules (Bell (1)). In addition, GPI LFA-3 would be expected to diffuse into the contact area during the duration of incubation to compensate for the depletion of free LFA-3 molecules in that region due to bond formation. This might in turn enhance further bond formation and redistribution of CD2 into the contact region. According to the fluid mosaic model advanced by Singer and Nicolson (32), the cell membranes may be viewed as two-dimensional viscous solutions of oriented globular proteins and lipids in instantaneous thermodynamic equilibrium. The redistribution of surface adhesion receptors by translational diffusion or by

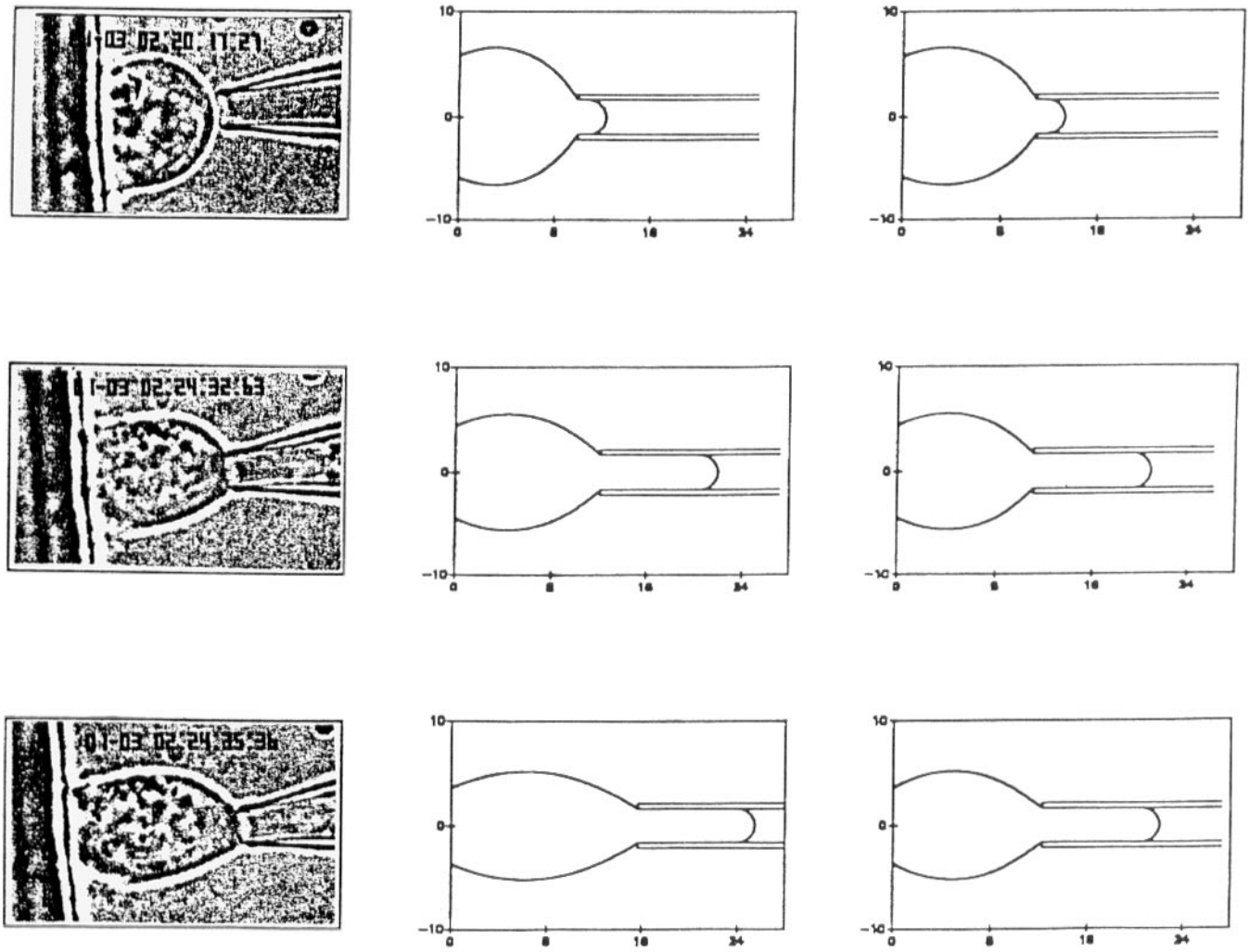

Figure 5. The modeled detachment by micromanipulation of a typical Jurkat cell from a planar bilayer containing GPI LFA-3. The experimental cell contours in column 1 belong to the micromanipulation events shown in Fig. 1 *A*. The corresponding contours predicted by models 1 (circumferential tension = 0) and 2 (circumferential tension = meridional tension) are shown in columns 1 and 2, respectively. Only part of the cell contour that remains between the planar bilayer and the tip of the pipette was computed. The cell projection inside the pipette was schematically drawn. The meridional tension at the tip of the pipette was assumed to be continuous. The equations of mechanical equilibrium for an axisymmetric membrane given by Timoshenko (38) were integrated analytically for the following specified boundary conditions: The radial dimension at the contact surface and the maximal radial dimension of the modeled cell are equal to the corresponding experimentally measured values. In addition, the predicted value of the angle the cell makes with the direction of the pipette at the edge of the pipette is set equal to the corresponding experimental value.

a metabolically driven process through the viscous membrane has since been demonstrated to be closely related to cell adhesion (7, 10, 21, 24).

Comparison of Micromanipulation Results with Other Data on Jurkat Cell–LFA-3 Interaction

Chan et al. (6) investigated the effects of the duration of incubation and the surface density of LFA-3 molecules on the percentage of Jurkat cells adhering to LFA-3-bearing surfaces by using plate inversion assays and laminar flow adhesion assays. The Jurkat cells were allowed to settle onto planar bilayers reconstituted with LFA-3 molecules for 1 h. These plates were then inverted for 1 h to detach unbound cells. Bound cells were measured by a fluorescence plate reader. Consistent with our findings, this study showed that Jurkat cells bound to the GPI isoform at site densities one order of magnitude lower than those required for binding to the TM isoform.

In laminar flow adhesion assays, Chan et al. (6) used fluid shear stress (0.5–16 dyn/cm^2) to detach the cells from the bottom of a rectangular chamber that had been coated with a planar bilayer. The cells were allowed to settle on the planar bilayer for 5 or 20 min before the application of shear stress. The percentage of cells that remained attached after the application of shear stress was found to decrease with the increasing fluid shear stress. The percentage of Jurkat cells that remained adhering to planar bilayers containing GPI LFA-3 after the application of laminar flow reached a peak at 5 min of incubation. The corresponding percentage was considerably less for TM LFA-3 under the same conditions. The difference between the shear resistances of cells adhering to the two isoforms of LFA-3 diminished towards zero,

however, as the duration of adhesion was increased to 20 min and the surface density of LFA-3 molecules was increased to 1,500 sites/μm^2.

Our experimental results are consistent with the flow chamber data obtained after 5 min incubation. The apparent discrepancy between micromanipulation data and flow chamber data for long durations of incubation may be due to statistical (single cell experiments vs. data on a cell population) as well as physical reasons. In laminar flow assays, the adhesion bonds between the cell and the substrate are sheared in response to the lateral force applied on the cell by the surrounding fluid. Furthermore, these bonds must generate an appropriate torque to balance the moment exerted by the fluid; i.e., some of these bonds must resist stresses in the direction normal to the contact plane. In micromanipulation experiments, on the other hand, the adhesion bonds located at the edge of conjugation experience significant axial stretching but little shearing. It is possible that the CD2-LFA-3 bonds resist against shear more efficiently than stretching. It should be of interest to explore this further in models and in experiments.

Conclusions

In this study, we characterized the direct contribution of CD2/LFA-3 interaction to the physical strength of Jurkat cell adhesion by using a micromanipulation method. Our technique enabled us to record the side views of Jurkat cells interacting with a planar substrate during the period of incubation and the subsequent forced detachment. In addition, we measured the minimum aspiration pressure needed to separate the cell from the planar substrate.

We showed that Jurkat T cells bound neither to clean glass washed with the medium, nor to planar bilayers that did not contain LFA-3 molecules. In contrast, Jurkat T cells adhered strongly to planar bilayers containing GPI LFA-3 (lipid-anchored isoform of LFA-3). The contact area between the cell and the substrate reached a maximum (20 μm^2) after 5–10 min of incubation. Jurkat cells in contact with a planar bilayer containing GPI LFA-3 at surface densities of 100–1,000 sites/μm^2 assumed approximately the shape of a liquid drop. The adhesive energy density between a Jurkat cell and a membrane coated glass chip containing 1,000 GPI LFA-3 molecules/μm^2 at the initial stage of detachment was $\sim$1/6 of the corresponding density between a cytotoxic T cell and its target cell (39). In cytotoxic T cell–target cell interaction, adherence strength increased during the course of cell detachment (34). Jurkat T cells, on the other hand, underwent extensive elongation in response to the pipette force. When the contact radius was reduced by $\sim$50%, the cell then detached quickly from its substrate.

We have also investigated the adhesion of Jurkat T cells to planar bilayers containing 1,000 TM LFA-3 (trans-membrane isoform of LFA-3) by using the same micromanipulation procedure. Our results showed that the pressure required to separate the Jurkat T cells from the planar bilayer containing TM LFA-3 was an order of magnitude smaller than that from the planar bilayer containing GPI LPA-3. The cells separated rapidly from the membrane-coated glass chip without a significant change in their approximately spherical cell shape. The TM and GPI isoforms of the LFA-3 molecule have comparable binding affinity to CD2 but different mobility: GPI LFA-3 is highly mobile within the lipid bilayer, while the TM LFA-3 is laterally immobile. The present findings illustrate the contribution of the CD2–LFA-3 interaction to the physical strength of T cell adhesion and the importance of receptor diffusivity on the strength of cell adhesion.

We would like to thank Dr. Richard Skalak for his useful suggestions in analysis of the data.

This research was supported by National Institutes of Health grants HL43026, CA31798, CA37955, and GM41460, and American Cancer Society grant IM-648.

Received for publication 4 March 1991 and in revised form 9 September 1991.

References

1. Bell, G. I. 1978. Models for the specific adhesion of cells to cells. *Science (Wash. DC).* 200:618–627.
2. Bell, G. I., M. Dembo, and P. Bongrand. 1984. Cell-cell adhesion: competition between nonspecific repulsion and specific bonding. *Biophys. J.* 45:1051–1064.
3. Brian, A. A., and H. M. McConnell. 1984. Allogeneic stimulation of cytotoxic T cells by supported planar bilayer. *Proc. Natl. Acad. Sci. USA.* 81:6159–6163.
4. Burridge, R., and J. B. Keller. 1978. Peeling, slipping and cracking—some one-dimensional free-boundary problems in mechanics. *SIAM Rev.* 20:31–61.
5. Carpen, O., M. L. Dustin, T. A. Springer, J. A. Swafford, L. A. Smith, and John P. Caulfield. 1991. Motility and ultrastructure of large granular lymphocytes on lipid bilayers reconstituted with adhesion receptors LFA-1, ICAM-1, and two isoforms of LFA-3. *J. Cell Biol.* 115:861–871.
6. Chan, P. Y., M. B. Lawrence, M. L. Dustin, L. Ferguson, D. Golan, and T. A. Springer. 1991. The influence of receptor lateral mobility on adhesion strengthening between membranes containing LFA-3 and CD2. *J. Cell Biol.* 115:245–256.
7. Chao, N.-M., S. Young, and M. M. Poo. 1981. Localization of cell membrane components by surface diffusion into a "trap". *Biophys. J.* 36:139–153.
8. Dembo, M., D. C. Torney, K. Saxman, and D. Hammer. 1988. The reaction limited kinetics of membrane to surface adhesion and detachment. *Proc. R. Soc.* B234:55–83.
9. Dong, C., R. Skalak, K. L. P. Sung, G. W. Schmid-Schonbein, and S. Chien. 1988. Passive deformation analysis of human leukocytes. *J. Biomech. Engn.* 110:27–36.
10. Duband, J.-L., G. H. Nuckolls, A. Ishihara, T. Hasegawa, K. M. Yamada, J. P. Thiery, and K. Jacobson. 1988. Fibronectin receptor exhibits high lateral mobility in embryonic locomoting cells but is immobile in focal contacts and fibrillar streaks in stationary cells. *J. Cell Biol.* 107:1385–1396.
11. Dustin, M. L., and T. A. Springer. 1989. T-cell receptor cross-linking transiently stimulates adhesiveness through LFA-1. *Nature (Lond.).* 341: 619–624.
12. Dustin, M. L., M. E. Sanders, S. Shaw, and T. A. Springer. 1987. Purified lymphocyte-function associated antigen-3 (LFA-3) binds to CD2 and mediates T-lymphocyte adhesion. *J. Exp. Med.* 165:677–692.
13. Dustin, M. L., P. Selvaraj, R. J. Mattaliano, and T. A. Springer. 1987. Anchoring mechanisms for LFA-3 cell adhesion glycoprotein at membrane surface. *Nature (Lond.).* 329:846–848.
14. Dustin, M. L., D. Olive, and T. A. Springer. 1989. Correlation of CD2 binding and functional properties of multimeric and monomeric lymphocyte function-associated antigen 3. *J. Exp. Med.* 169:503–517.
15. Evans, E. A. 1989. Force between surfaces that confine a polymer solution: derivation from self-consistent field theories. *Macromolecules.* 22:2277–2286.
16. Evans, E. A., and K. Baxbaum. 1981. Affinity of red blood cell membrane for particle surface measured by the extent of particle encapsulation. *Biophys. J.* 34:1–12.
17. Evans, E. A., and A. Leung. 1984. Adhesivity and rigidity of erythrocyte membrane in relation to wheat germ agglutinin in binding. *J. Cell Biol.* 98:1201–1208.
18. Evans, E., and A. Yeung. 1989. The effective viscosity and the cortical tension of blood granulocytes determined by micropipette aspiration. *Biophys. J.* 56:151–160.
19. Hollander, N., P. Selvaraj, and T. A. Springer. 1988. Biosynthesis and function of LFA-3 in human mutant cells deficient in phosphatidylinositol-anchored proteins. *J. Immunol.* 141:4283–4290.
20. Johnson, K. L. 1975. Contact Mechanics. Cambridge University Press, New York. 452 pp.
21. Kupfer, A., and S. J. Singer. 1989. Cell Biology of cytotoxic and helper T cell functions. Immunofluorescence microscopic studies of single cells and cell couples. *Annu. Rev. Immunol.* 7:309–337.

22. Lawrence, M. B., and T. A. Springer. 1991. Leukocytes roll on a selectin at physiological flow rates: distinction from the prerequisite for adhesion through integrins. *Cell.* 65:859–873.
23. McClay, D. R., and C. A. Ettensohn. 1987. Cell adhesion in morphogenesis. *Annu. Rev. Cell Biol.* 3:319–345.
24. McCloskey, M. A., and M. M. Poo. 1986. Contact-induced redistribution of specific membrane components: local accumulation and development of adhesion. *J. Cell Biol.* 102:2185–2196.
25. McConnell, H. M., T. H. Watts, R. M. Weis, and A. A. Brian. 1986. Supported planar bilayer in studies of cell-cell recognition in the immune system. *Biochem. Biophys. Acta.* 864:95–106.
26. Mohandas, N., R. M. Hochmuth, and E. E. Spaeth. 1974. Adhesion of red cells to foreign surfaces in the presence of flow. *J. Biomed. Mater. Res.* 8:119–136.
27. Plunkett, M. L., and T. A. Springer. 1986. Purification and characterization of the lymphocyte function-associated-2 (LFA-2) molecule. *J. Immunol.* B6:4181–4188.
28. Qallik, S., Usami, S., K. M. Jan, and S. Chien. 1989. Shear stress induced detachment of human polymorphonuclear leukocyte from endothelial cell monolayers. *Biorheology.* 26:823–834.
29. Rouslahti, E., and M. D. Pierschbacher. 1987. New perspectives in cell adhesion: RGD and integrins. *Science (Wash. DC).* 238:491–497.
30. Selvaraj, P., M. L. Dustin, R. Mitnacht, T. Hünig, T. A. Springer, and M. L. Plunkett. 1987. Rosetting of human T-lymphocytes with sheep and human erythrocytes. *J. Immunol.* 138:2690–2695.
31. Shaw, S., G. E. Ginther Luce, R. Quinones, R. E. Gress, T. A. Springer, and M. E. Sanders. 1986. Two antigen-independent adhesion pathways used by human cytotoxic R-cell clones. *Nature (Lond.).* 323:262–264.
32. Singer, S. J., and G. L. Nicolson. 1972. The fluid mosaic model of the structure of cell membranes. *Science (Wash. DC).* 175:720–731.
33. Springer, T. A. 1990. Adhesion receptors of the immune system. *Nature (Lond.).* 346:425–434.
34. Sung, K. L. P., L. A. Sung, M. Crimmins, S. J. Burakoff, and S. Chien. 1986. Determination of junction avidity of cytotoxic T-cell and target cell. *Science (Wash. DC).* 234:1405–1408.
35. Sung, K.-L. P., C. Dong, G. W. Schmid-Schönbein, S. Chien, and R. Skalak. 1988. Leukocyte relaxation properties. *Biophys. J.* 54:331–336.
36. Sung, K.-L. P., L. A. Sung, M. Crimmins, S. J. Burakoff, and S. Chien. 1988. Dynamic changes in viscoelastic properties in cytotoxic T-lymphocyte–mediated killing. *J. Cell Sci.* 91:179–189.
37. Tanun, L. K. 1988. Lateral diffusion and fluorescence microscope studies on a monoclonal antibody specifically bound to supported bilayers. *Biochemistry.* 27:1450–1457.
38. Timoshenko, S. 1940. Theory of Plates and Shells. McGraw Hill Co., New York. 580 pp.
39. Tözeren, A. 1989. Adhesion induced by mobile crossbridges: steady state peeling of conjugated cell pairs. *J. Theor. Biol.* 140:1–17.
40. Tözeren, A., K. L. P. Sung, and S. Chien. 1989. Theoretical and experimental studies on crossbridge migration during cell dissagregation. *Biophys. J.* 55:479–487.